Available online at www.sciencedirect.com

ScienceDirect

Energy Procedia 81 (2015) 883 – 896

Energy Procedia

69th Conference of the Italian Thermal Engineering Association, ATI 2014

Numerical analysis of methane direct injection in a single-cylinder 250 cm^3 spark ignition engine

Stefania Zanforlin[a,*] and Alberto Boretti

[a] *Assistant Professor, Department of Energy, Systems, Territory and Constructions Engineering, University of Pisa, l.go Lucio Lazzarino, 56122 Pisa, Italy*

Abstract

The paper shows the results of the numerical tasks of a study aimed to evaluate the potential of low-pressure (< 20 bar) direct injection systems for internal combustion engines fed with gaseous fuels. Starting from the geometry of a low-cost commercial injector already available for GDI uses, a 2D axisymmetric CFD analyses is performed to assess the influence of injection pressure and valve and seat-valve profiles on jet characteristics, methane-air mixing, and charge distribution at ignition time. Then 3D simulations for the motorcycle single cylinder test-engine are carried out considering as much as possible combustion chamber details and realistic boundary conditions. Although it is possible identifying which operating and geometrical details of injection system are able to support complete mixture homogeneity, this study shows tremendous difficulties, in case of gaseous fuels, to realise satisfactory stratification charges that would be required to obtain satisfactory performance at partial loads.

Peer-review under responsibility of the Scientific Committee of ATI 2014

Keywords: Direct injection, gas engine, methane, spark ignition, poppet valve, outward opening, CFD.

Biographical

Dr. Alberto Boretti has been senior researcher and manager in the automotive industry for about 20 year and associate and research professor of engineering mechanical and automotive in the academy for 6 years. He is the author of more than 240 peer review papers, 2 books and 3 book chapters. He has been working on CFD since 1983 covering many different applications. Dr. Stefania Zanforlin is Assistant Professor in Fluid Machinery at the University of Pisa. She has an MSc degree in Chemical Engineering and a PhD in Energetics. She has 18 years of experience in CFD tools

* Corresponding author. Tel.: +39-050-2217145; fax: +39-050-2217150.
E-mail addresses: a.a.boretti@gmail.com (A. Boretti), s.zanforlin@ing.unipi.it (S. Zanforlin)

Peer-review under responsibility of the Scientific Committee of ATI 2014
doi:10.1016/j.egypro.2015.12.142

applied to internal combustion flows (reciprocating engines) and external flows (wind turbines). She is author of about 40 papers concerning internal combustion engine investigations: Diesel combustion modelling; fluid dynamics of charge stratification in gasoline direct injection engines; direct injection systems for engines fed with hydrogen and natural gas.

1. Introduction

In the recent years, even more attention is paid to alternative fuels which can agree to both reducing the fuel consumption and the pollutant emissions.
Large bore spark ignited engines for power generation fed with natural gas, bio-gas or syngas entail high thermal efficiency by adopting lean-burn premixed strategy, turbocharging and Miller cycle [1]; natural gas and bio-gas ignition is usually achieved by mean pilot ignition in a pre-chamber [2], syngas does not need it because of the satisfactory ignition and combustion properties of hydrogen that is one of the syngas components [3].
Among gaseous fuels, Compressed Natural Gas (CNG, which is made by ~ 96% of methane) and bio-methane are considered two of the most interesting in terms of engine vehicular application. They represents an immediate advantage over other hydrocarbon fuels leading to lower CO_2 emissions tanks to their lower carbon content. Compared to gasoline, CH_4 has wider flammable limits and better anti-knock properties, yet lower flame speed that could be enhanced by adding small amount of hydrogen [4, 5]. Moreover, CNG is affordable and available worldwide.
Usually, CNG engines are developed by integrating CNG injectors in the intake manifold of a baseline gasoline engine, thereby remaining gasoline compliant. However, this does not lead to a bi-fuel engine but instead to a compromised solution for both gasoline and CNG operation.
Direct Injection (DI) provides higher volumetric energy of the mixture and therefore higher engine specific power; moreover the in-cylinder gas injection and post-expansion lead to the mixture temperature decreasing that allows higher boost pressure and higher efficiency. In the last decade sophisticated high-pressure systems have been developed [6] that properly agree to the homogeneous mixture requirements of full load operation. However, high-pressure injection systems are penalised by a low range or by the need of an on-board re-compression system.
DI would give the maximum advantages with respect to Port Fuel Injection (PFI) at partial loads if it could generate proper fuel stratification that, independently of the fuel (liquid or gaseous), increases efficiency, decreases cooling losses, extends lean operation rage and reduces cycle-to-cycle variation [7]. Charge stratification is a challenging task in case of gaseous fuels, indeed extreme difficulties occur when conventional approaches (efficacious enough for gasoline) are adopted: auto-confining injectors, piston bowls or air-wall guided methods. Recent studies focused on medium-high injection pressure demonstrated in some measure acceptable results [8, 9].
The present research is motivated by the actual trend of the increasing use of gaseous fuels, and by the need to study and develop simple, reliable and less expensive injection systems; since medium-low pressures should be preferable also to extend the vehicle range (by means a more complete use of the on-board storage tank) we assumed injection pressures below 20 bar.
Our main objective is to contribute to achieve a deep insight into the physical mechanisms involved in the gaseous injection and in-cylinder mixing processes and to understand how the injection system geometrical details and the operating pressure can determine homogeneous or stratified charge characteristics.

Nomenclature

Φ	equivalence ratio = $(air/fuel)_{actual}/(air/fuel)_{stoichiometric}$	EVC	Exhaust Valve Closing
ATDC	After Top Dead Centre	IVC	Intake Valve Closure
BDC	Bottom Dead Centre	IVO	Intake Valve Opening
BTDC	Before Top Dead Centre	PFI	Port Fuel Injection
CA	Crank Angle	RPM	Revolution Per Minute
CNG	Compressed Natural Gas	SI	Spark Ignition
COV	Coefficient Of Variation	SOI	Start Of Injection
DI	Direct Injection	TDC	Top Dead Centre

2. Test engine

A research is carrying out that include numerical and experimental analysis on medium-low injection pressure DI systems for gaseous fuels. The study is based on a commercial 250 cm^3 single-cylinder spark ignition four-stroke engine (Piaggio Beverly) representative of the most popular two-wheel vehicles in Europe. A version equipped with an optical window on a flat piston is also available to analyse the combustion process with high spatial and temporal resolution. The engine is originally equipped with a GDI system that is replaced with an injector suitable for methane. A commercial air-assisted outward-opening GDI injector (Synerject Strata, Figure 2.1) is easily adapted to be used with methane by removing the components originally dedicated to gasoline and using the air unit (characterised by large efflux areas) to admit the gaseous fuel. Nozzle tip lift and geometry details of the injector interior necessary to design the computational grid are found in literature [10, 11].

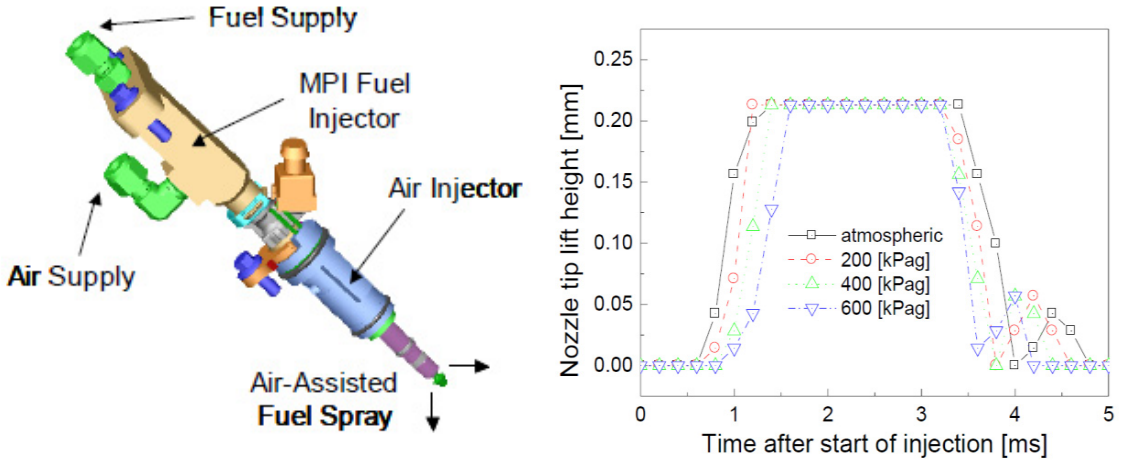

Figure 2.1: Main components of the original Synerject Strata GDI injector (left); original injector valve lift versus time as found in literature [10] (right).

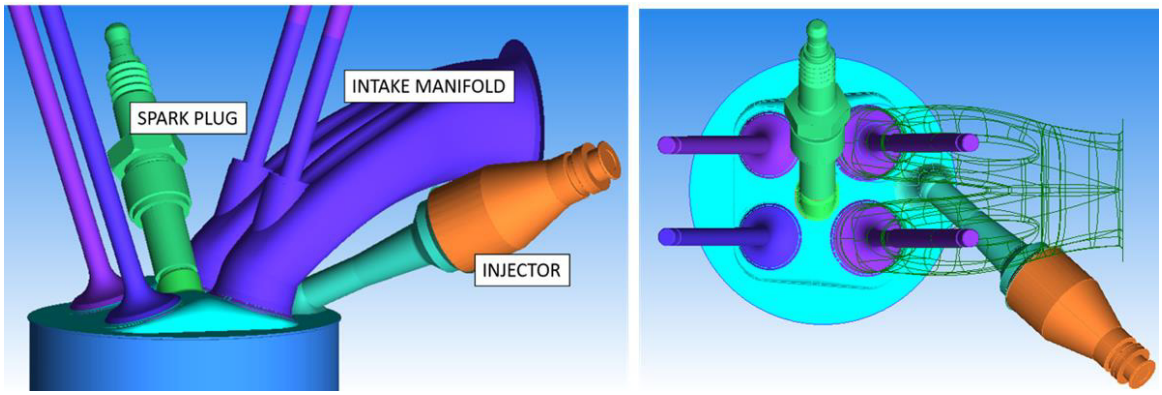

Figure 2.2: Overall arrangements of engine head with valves, intake ducts, spark plug, and original GDI injector system.

The test engine arrangement shown Figure 2.2 results strongly affected by some original engine constrains, in particular: (a) the peripheral location of injector together with its axis orientation lead to the fuel spreading on the head surface and on the cylinder liner (the problem arises with gaseous fuels, as will be discussed in chapter 5); (b) as it usually occurs in high performance motorcycle engines, intake valves close with a high crank angle delay with respect to BDC, retarding the beginning of injection and consequently shortening the time available for in-cylinder fuel-air mixing.

3. Methodological approach

The numerical study is performed in two steps: a 2D axisymmetric analysis of the injection and fuel-air mixing mechanisms; a 3D investigation of the injector behaviour when located in the real prototype engine. AVL-Fire code is adopted, a general fluid flow solver employing the finite volume discretisation method resting on integral conservation statements applied to a general polyhedral control volume. Since it is conceived to deal internal combustion engine analysis, it is able of handling models including an arbitrary number of moving boundaries. To solve the linear systems pre-conditioned conjugate gradient methods are applied. The k-ζ-f turbulence model is chosen, which is based on Durbin's elliptic relaxation concept [12, 13]. Although the calculation time is 15% more than k-e model, the k-ζ-f model is more robust, more stable and less sensitive to non-uniformity and clustering of the computational grid [14]. AVL-Fire is able to run with both structured and unstructured grids. Multi-block grids are created, making extensive use of the "O-grid" technique, where all the single blocks are structured, while the domain as a whole is unstructured. This improves grid quality and allows the concentration of cells in areas that require high resolution (for instance, the area downstream of the injection valve and the area around spark plug). An example of grid used for 2D simulations is shown in Figure 3.1. The engine head profile is simplified (real 4-stroke engines don't have a symmetrical head) only including a domed shape and a squish crown at the cylinder periphery; yet the combustion chamber volume agrees to the actual engine compression ratio. An example of grid is shown in figure 3.1. The overall elements number is ~ 45.000. To accommodate the motion of piston and injector valve a sequence of 4 grids is used.

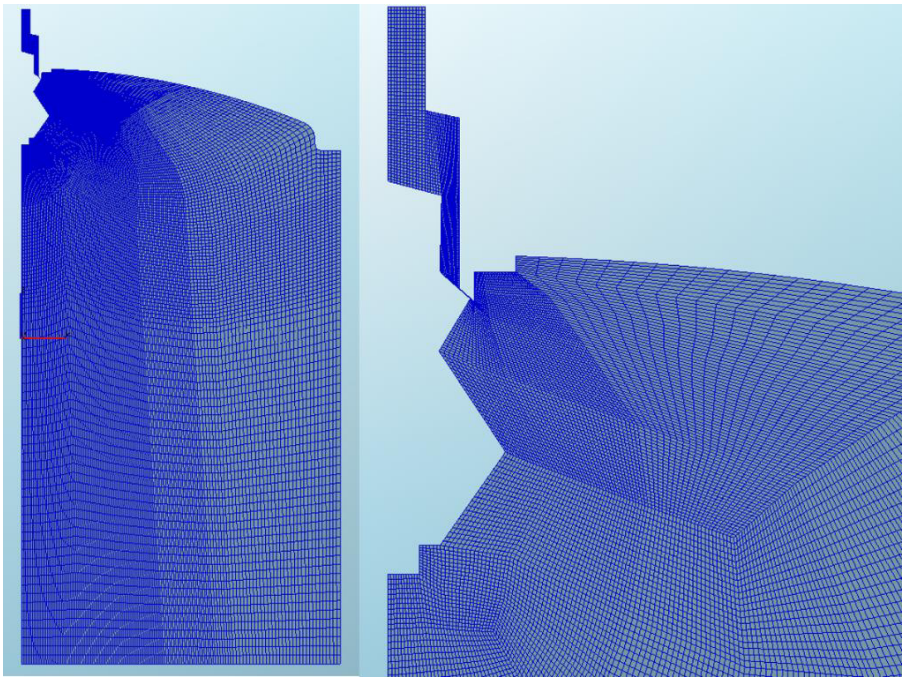

Figure 3.1: Grid for the 2D axisymmetric simulations concerning the original Synerject injector (on the left); grid details in the injector region (on the right).

In most of our operating conditions the pressure expansion ratio is higher than the critical value (that is ~ 1.9), thus post-expansion occurs at the exit of the injection valve and high grid resolution in the valve region is required to accurately capture the transient jet evolution details that govern the fuel-air mixing [15, 16]. Indeed, with injection pressure enough high the emerging jet reaches velocities locally supersonic and the flow downstream the nozzle is repeatedly accelerated and decelerated due to the complex rarefaction and compression waves which result [17]. The phenomenon is visible in Figure 3.2 for a methane injection pressure of 18 bar. For 2D cases simulations start at the

intake valve closure (IVC); initial flow-field is set quiescent, since intake air motion is not considered.
Since the experimental test-rig is not already completely equipped at this time, the preliminary validation of the numerical models is performed on the base of the numerical and experimental results found in a study dealing with the DI injection of natural gas by means a poppet valve in a large bore engine [15]; a satisfactory agreement is achieved between our CFD results and those data.
Figure 3.3 shows the engine grid at BDC; due to the particular injector orientation the domain is not symmetrical and therefore the whole engine volume needs to be considered, greatly increasing computation efforts. For the simulations, that cover the range from the end of the exhaust phase to the ignition time, a sequence of 8 grids, whose size range from 350000 to 700000 cells, is generated.
To limit the number of structured blocks, and therefore the grid generation effort, the computational grid neglects exhaust valves, therefore the first part of the intake stroke corresponding to the overlap is neglected, as well as the flow inside the exhaust ducts; thus computations started at EVC. It is well know that also the exhaust stroke should be considered to correctly describe the actual flow field in the cylinder during intake and compression; however the mentioned simplifications do not lead to significant inaccuracies as regards the investigated phenomena. However, all head details that affect the flow field evolution during compression (including the spark-plug) are taken into account.

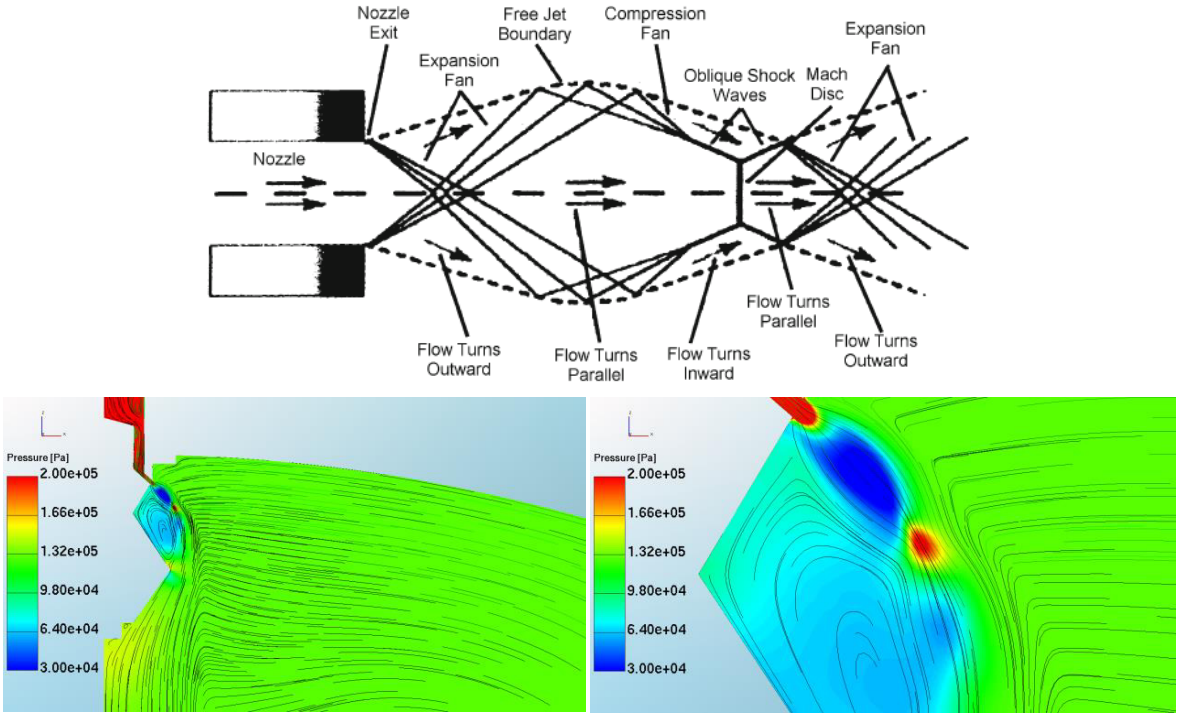

Figure 3.2: Schematic representation on an under-expanded jet structure (top); streamlines and pressure map obtained with the original Synerject injector and an injection pressure of 18 bar (bottom left); details (bottom right).

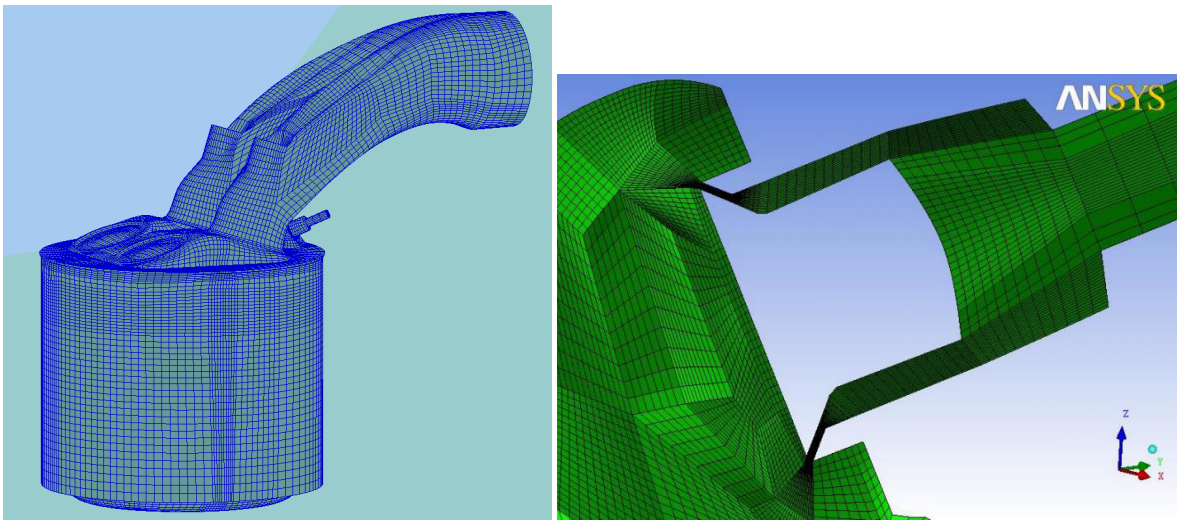

Figure 3.3: 3D structured grid of the prototype engine (left); details of the structured grid around the injection valve (right).

Initial conditions inside cylinder and intake ducts, as well as inlet air pressure boundary conditions are obtained from 1D engine-cycle simulations, performed by means of AVL-Boost software. The Boost model is set using cylinder pressure data experimentally obtained running the engine with gasoline.
As will be explained in chapter 5, unsatisfactory mixture homogeneity is predicted when assuming the original injection configuration. To overcome this drawback the new component shown in Figure 3.4 is designed; it consists in a conical-cylindrical nozzle positioned at the injector end to deviate the emerging jet towards the cylinder axis.

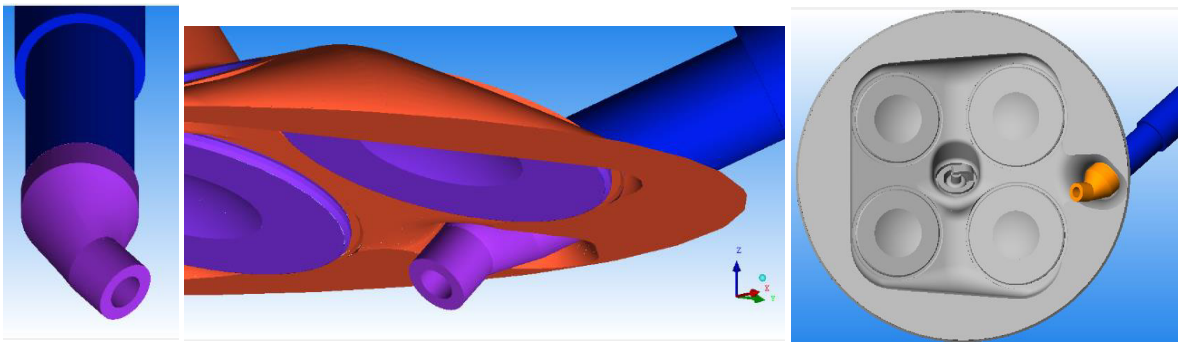

Figure 3.4: Design of the new component used to divert the jet towards the cylinder axis (left); global engine head arrangement with the new component positioned at the injector exit (centre and right).

Since the additional nozzle involves additional difficulties in generating a completely structured multi-block grid, an unstructured grid is realised for the combustion chamber, still keeping structured the volumes (cylinder and piston bowl, injector interior and nozzle efflux volume) containing mobile surfaces to better accomplish their motion. The new hybrid mesh is shown in Figure 3.5.
To check the influence of cell number on computational results, the hybrid mesh is realised in two versions: a coarse grid of about 350000 elements and a finer grid of about $1.0*10^6$ elements most of them distributed in the combustion chamber, in particular in the efflux zone downstream the nozzle (Figure 3.6).

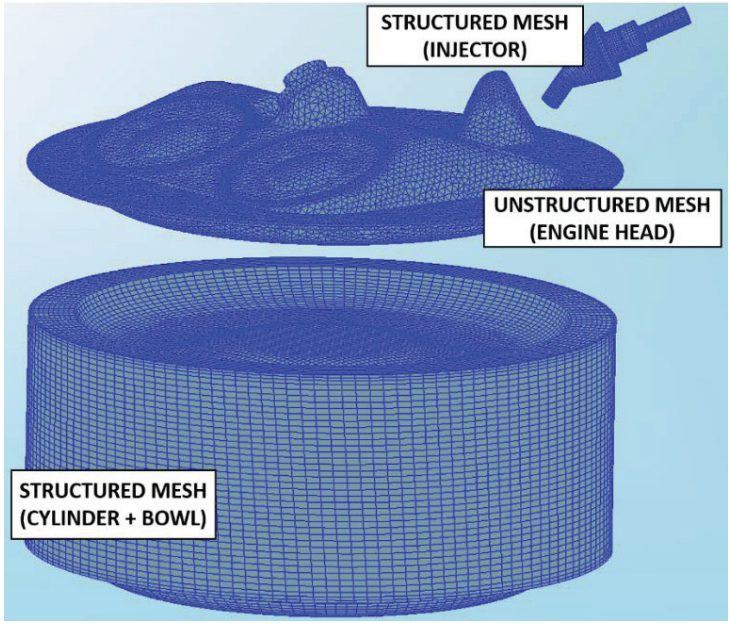

Figure 3.5: Structured multi-block grid of cylinder, piston bowl, injector interior, additional nozzle, and unstructured grid of combustion chamber.

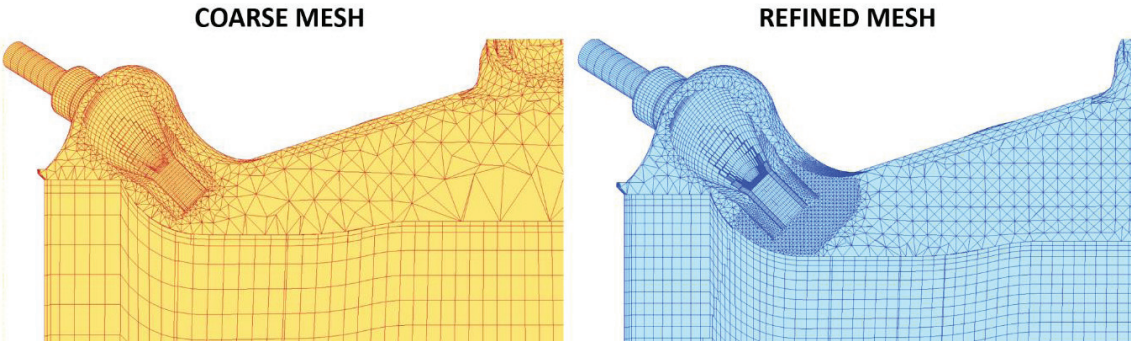

Figure 3.6: Details of the coarse grid (~350000 elements) and of the finer grid (~$1.0*10^6$ elements) in the injection zone.

4. 2D analyses of injection and mixing processes

Two pressure levels are investigated: 6 bar that is the original air delivery pressure; 18 bar that is indicative of a medium injection pressure (the only necessary modification to the injection system is to the spring preload). All CFD simulations are done at 2500 RPM; despite this engine speed is more interesting for stationary use than for vehicles, it is chosen since the injection time can be sufficient to deliver a significant amount of fuel also with low injection pressure (at 6 bar, $\Phi \leq 0.65$ are achievable), the limit being the efflux area of injector. Pressure and temperature at the simulation beginning are 1.2 bar and 340 K. The effects of injection pressure and timing on mixing completeness predicted at high load for the original injector are visible in Figure 4.1. In all the chapter figures giving the methane mass distribution, the mass fraction ranges from 0 (blue) to twice the mean fraction obtained for each simulation (red).

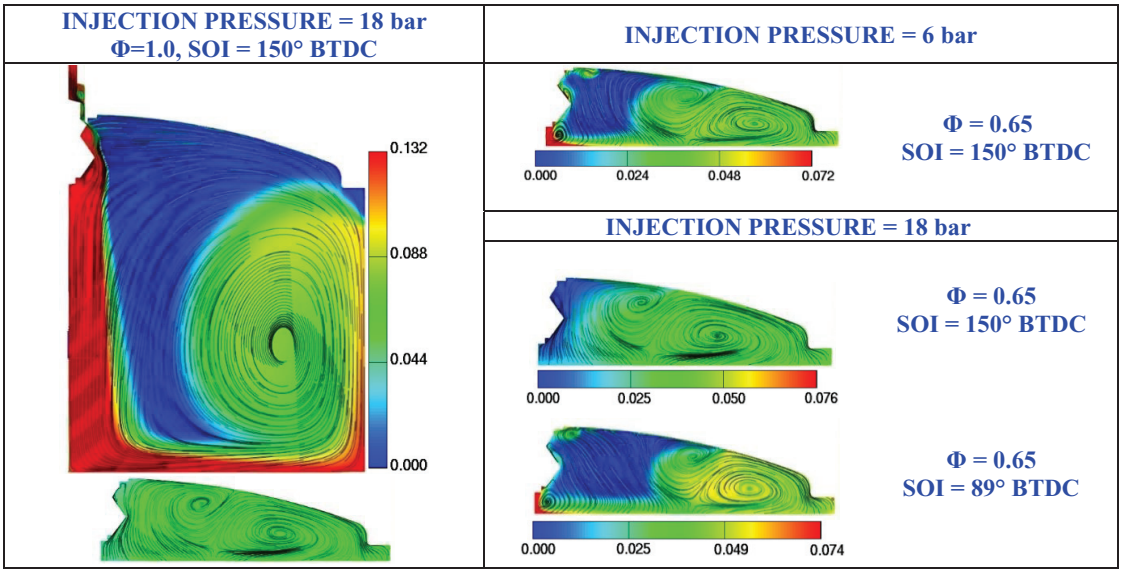

Figure 4.1: Jet shape of the original injector (top left); streamlines and CH_4 mass fraction at ignition time (15° BTDC) predicted with 18 bar and 6 bar of injection pressure, and for two Start Of Injection (SOI = 150° and 89° BTDC).

The fuel jet emerging from the small valve annular orifice exhibits a very narrow cone angle and therefore an high momentum that leads to a vigorous impingement on piston surface: the impingement and the subsequent wall-spreading process support fuel-air mixing, that appears complete at ignition time for full load (Φ=1.0) when injection starts enough early (at IVC, i.e. 150° BTDC; Figure 4.1 on the left). To check the effects of injection pressure a fuel amount corresponding to an average Φ of 0.65 is set (the maximum achievable at 6 bar); with 6 bar a SOI of 150° BTDC is adopted, whereas with 18 bar two SOI are set: 150° BTDC, and 89° BTDC that implies to finish the injection at the same CA of 6 bar. Results depicted in Figure 4.1 (on the right) suggest that it is the time available for mixing, more than the injection pressure level, the main parameter that determines the charge homogeneity characteristics at ignition time.
The geometrical modifications to the injection system listed in Figure 4.1 are investigated with the aim of find out solutions that support the fuel-air mixing or the charge stratification.

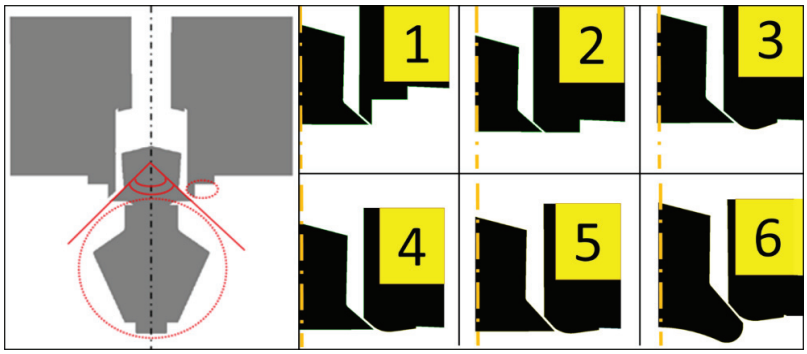

Figure 4.2: Original injector design [10] with geometrical parameters that have been investigated: valve protrusion, valve-cone angle, seat-valve characteristics (left); list of modifications to the original injector system geometry (right).

In geometry (1) the injector tip protrusion is removed. The manufacturer declares that the protrusion helps to stabilise

the gasoline plume when operating conditions changing: first we verified if it is useful for methane too. Results are not shown for briefly, since they are almost the same obtained with the original Synerject injector.
In geometry (2) the valve-seat does not penetrate in the combustion chamber, thus the fuel jet emerges quite close to the head walls. The proximity of walls affects the jet behaviour as depicted in Figure 4.2: during the first part of injection (high ratio of the supply pressure to the cylinder pressure) a compact conical jet occurs, whereas during the last part of injection (low pressure ratio) the fuel spreads on the head walls. The occurring of both these mechanisms support the mixing.
Geometry (3) is derived from (2) adding a deep round (protruded in the combustion chamber) to the periphery of the valve-seat in order to induce a very different jet behaviour; as shown in Figure 4.3, with 18 bar (high pressure ratio) a narrow conical jet is obtained, whereas with 6 bar (low pressure ratio) the fuel spreads on head wall due to the Coandă effect, the tendency of a fluid jet to be attracted to a nearby surface.

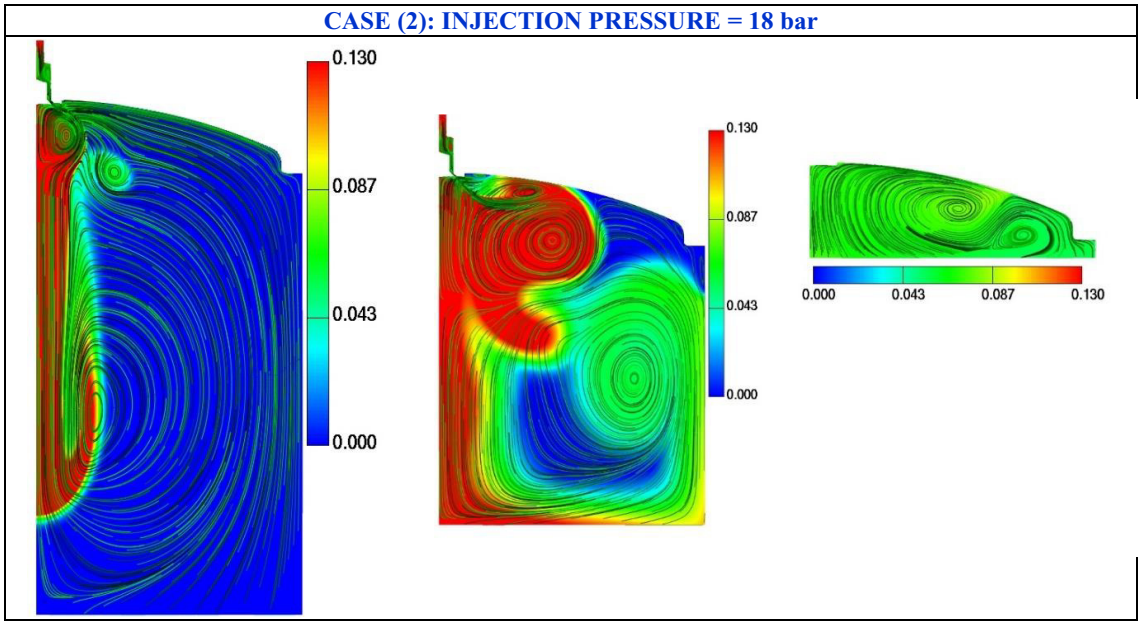

Figure 4.3: Streamlines and fuel mass fraction for case (2) at full load and 18 bar of injection pressure (140°, 90° and 15° BTDC).

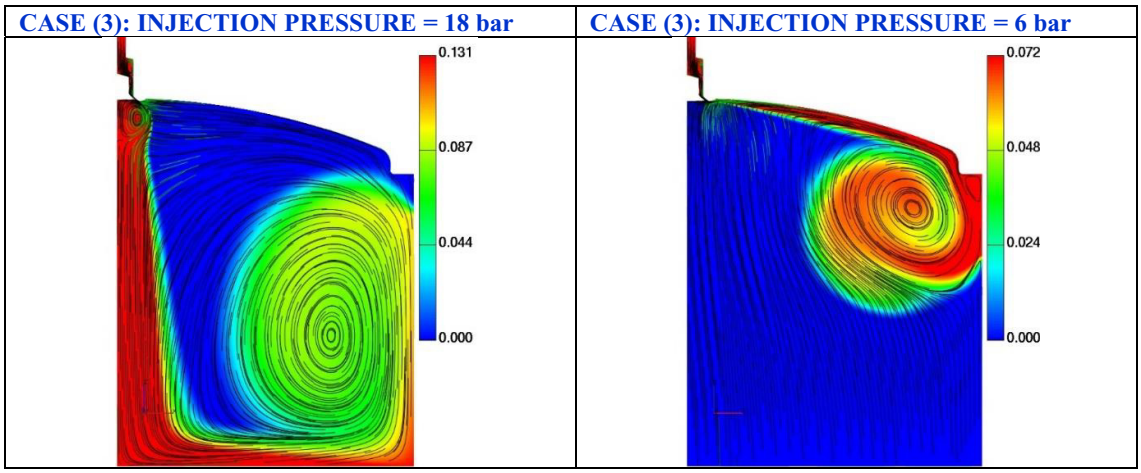

Figure 4.4: Streamlines and fuel mass fraction predicted for case (3) at 90° BTDC: full load and 18 bar (left); Φ=0.65 and 6 bar (right).

Geometry (4) is obtained from (3) by enlarge the round radius, making the round more mild and also less protruded in the combustion chamber; a more unstable jet is obtained with the same behaviour observed in case (2). Also in this case the mixing results complete, as can be seen in Figure 4.4.

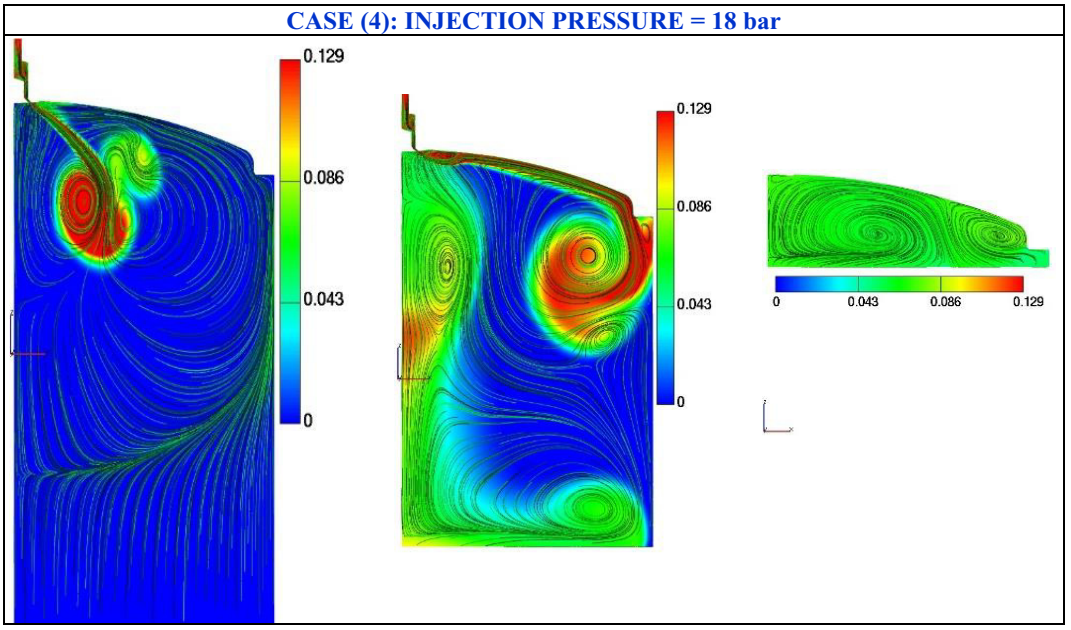

Figure 4.5: Streamlines and fuel mass fraction predicted for case (4) at full load and 18 bar of injection pressure (140°, 90° and 15° BTDC).

Geometry (5) has a narrower valve cone angle (84°) and even a milder round: a well-defined and stable Coandă effect occurs leading to an unsatisfactory mixing at ignition time (Figure 4.5).
Geometry (6) is similar to (5): with 18 bar, and during the first part of injection in case of 6 bar, the rounded valve-seat periphery induces the fuel spreading on the head wall. But, with 6 bar, during the last past of injection the narrower valve cone angle (80°) and the valve bottom profile generate a conical compact jet (Figure 4.6). This interesting behaviour suggests that also with a medium injection pressure (18 bar) geometry (6) could be adopted (together with a piston bowl to better confine the fuel) to achieve a certain stratification, or fuel enrichment, just delaying the injection to reduce pressure ratio; more study is need.

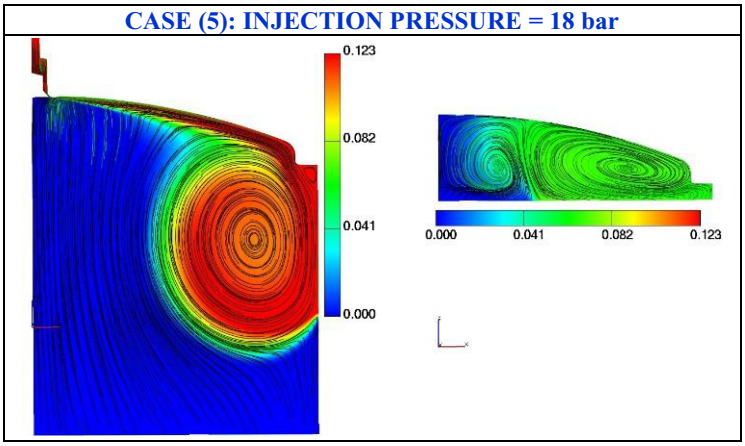

Figure 4.6: Streamlines and fuel mass fraction predicted for case (5) at full load and 18 bar of injection pressure (90° and 15° BTDC).

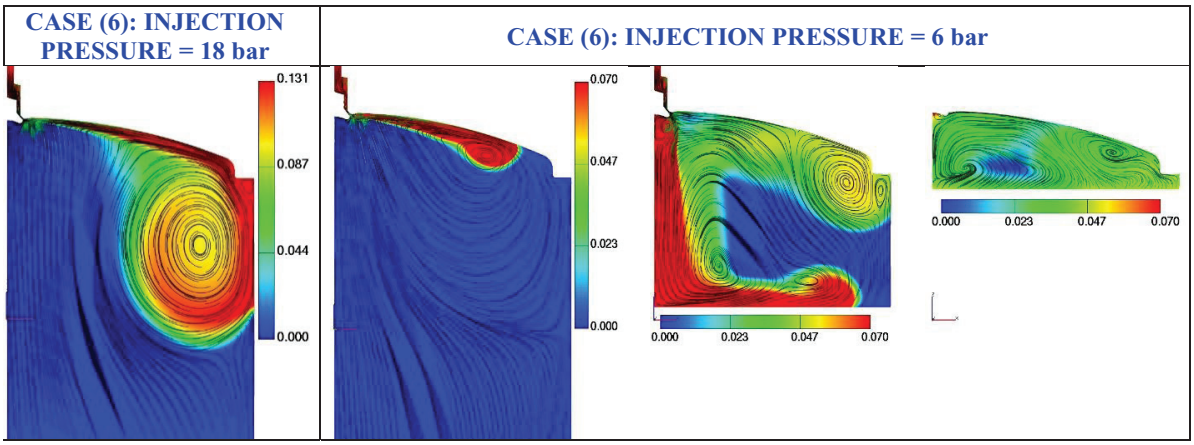

Figure 4.7: Streamlines and fuel mass fraction for case (6): full load and 18 bar (100° BTDC, right); Φ=0.65 and 6 bar (135°, 60°, 15° BTDC, left).

5. 3D investigations of injection and mixing in the real engine

At first the behaviour of the Synerject injector (without the protrusion) located in the placement of the original GDI system of the real engine is investigated for both 18 and 6 bar of injection pressures. As can be seen in Figures 5.1 and 5.2, for all the examined operating conditions the particular injector axis orientation addresses the fuel towards the head and cylinder-liner walls. An ineffective mixing process, based on on-wall spreading, takes place that leads to a lake of fuel in the spark plug region at the ignition time (15° BTDC).

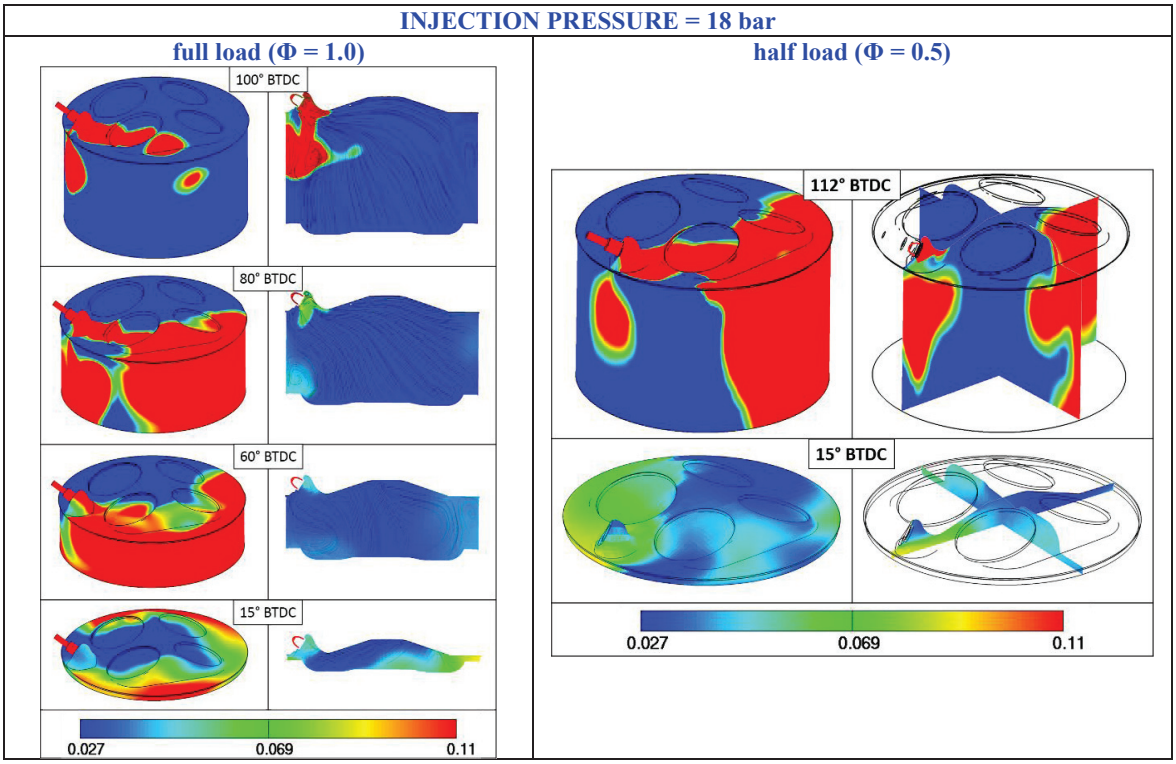

Figure 5.1: fuel mass fraction distribution predicted with the original injector, for full and half loads, 18 bar of injection pressure, SOI=150° BTDC.

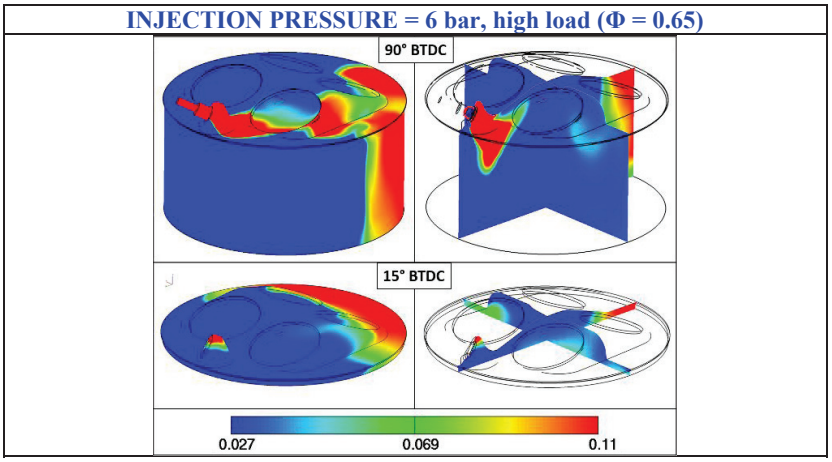

Figure 5.2: fuel mass fraction distribution predicted with the original injector, for high load (Φ=0.65), 6 bar of injection pressure, SOI = 150° BTDC.

The addition of a nozzle at the injector exit greatly helps to overcome the problem, as shown in Figure 5.3: now the fuel jet is directed on the piston surface; the impingement and wall-spreading processes support the achievement of a flammable mixture. Also at partial load (Φ=0.5) the methane mass fraction results inside the flammability range, however the charge cannot be considered correctly stratified, since most of the fuel appears located at the periphery of the combustion chamber.

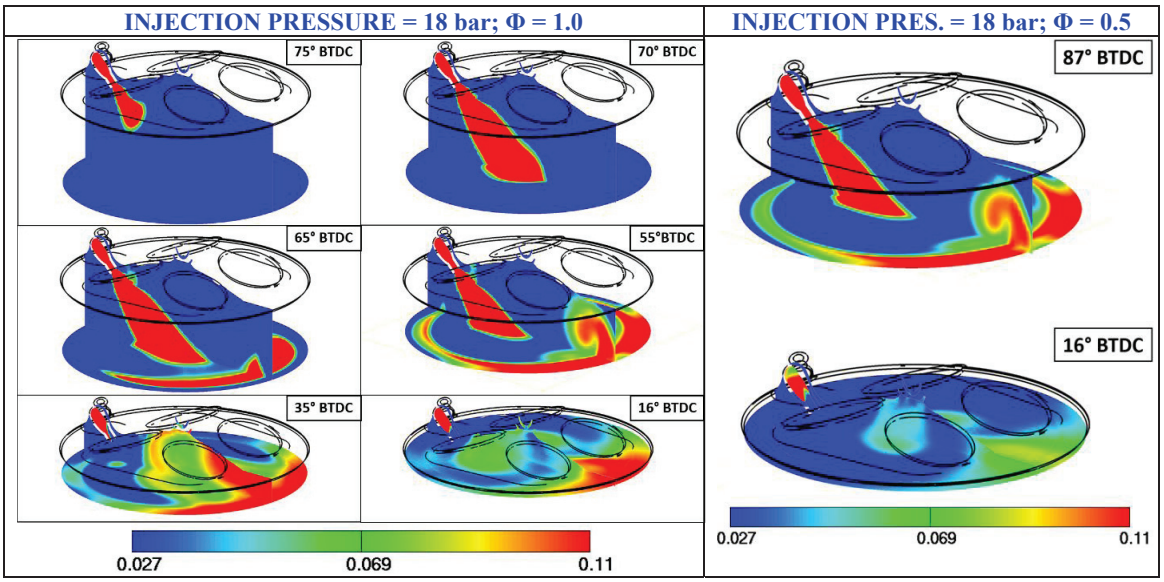

Figure 5.3: fuel mass fraction distribution predicted with the additional nozzle for 18 bar of injection pressure, SOI = 150° BTDC, Φ=1.0 (on the left), and Φ=0.5 (on the right).

In Figure 5.4 jet and mixing evolution, together with pressure maps in the injection zone, obtained with the fine ($1.0*10^6$ elements) and the coarse (350000 elements) grids are compared; the operating conditions are full load and 18 bar of injection pressure. With the finer grid the small cell sizes, especially in the efflux zone downstream the nozzle, allow to accurately predicting even the compression and rarefaction flow phenomena that are typical of an

under-expanded jet. Not substantial differences are noticeable for the two grids with respect to jet penetration and mixing features, however at the ignition time a difference of 7% is found for the methane average fraction in the small volume around the spark plug.

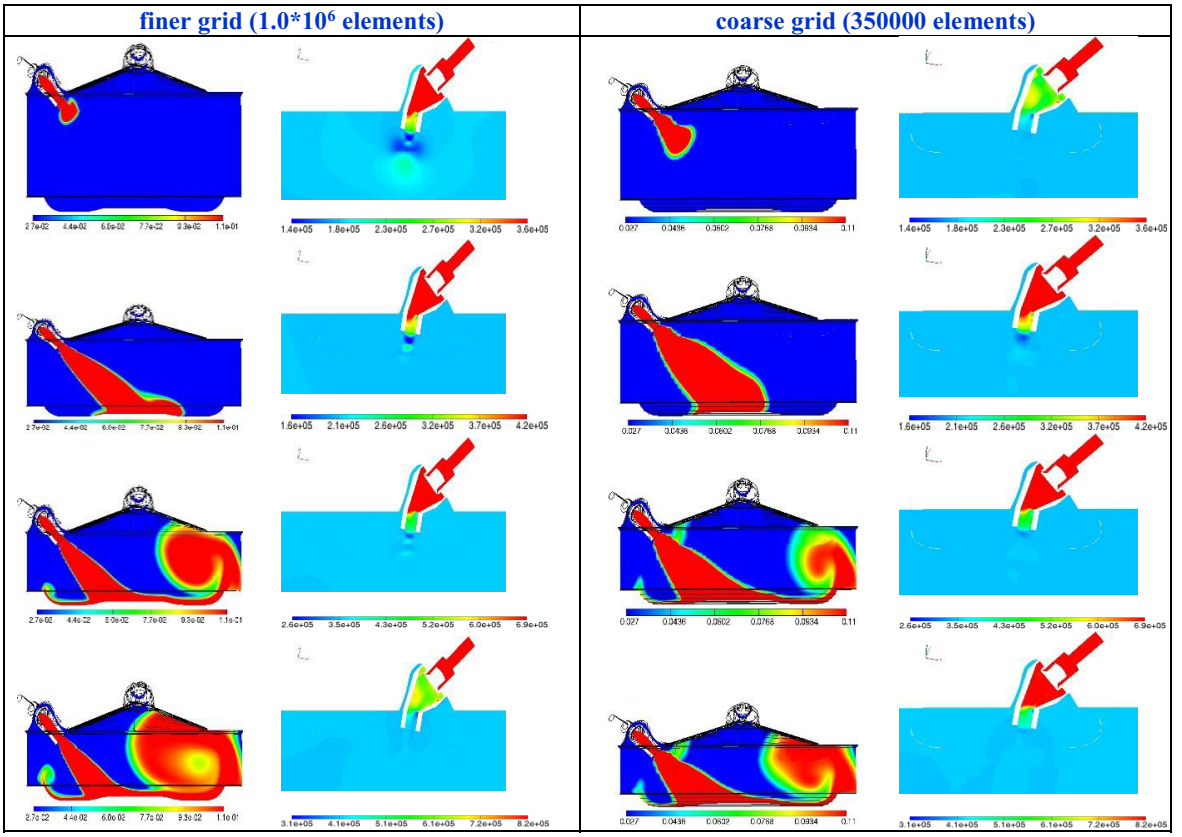

Figure 5.4: fuel mass fraction distribution and pressure map in the injection zone predicted with the finer and the coarse grids for full load (18 bar).

6. Discussion and Conclusions

The analysis of the injection process, performed in 2D to short calculation times even with very small cells, shows that the main parameters determining the type of flow emerging from the injector, and therefore the mixing mechanisms, are pressure expansion ratio (i.e., the ratio of the supply pressure to the cylinder pressure) and injection valve and valve-seat geometry. Two principal jet evolution and mixing mechanisms can occur: a mixing process mainly governed by the impingement of a high momentum jet on the piston top; fuel spreading and sliding on the walls due to the Coandă effect. Only the former leads to a satisfactory charge homogeneity (if the time available for mixing is sufficient) since it produces more vigorous vortex structures as well as more substantial gas flow along the piston surface and cylinder wall [15]. Combining some geometrical details to a low pressure ratio (obtainable by mean a delay of the injection timing) it is even possible to get a sequence of both the mechanisms that could be efficaciously used to achieve a certain stratification. However the investigation results suggest that it is extremely difficult to properly confine a gaseous fuel.

If charge stratification is impractical, as good as possible charge homogeneity becomes desirable at ignition time for the whole engine operating range. 3D investigations of injection and mixing in the real engine allow to predict a poor charge homogenisation with a fuel lake in the spark plug region, originated from some constrains in the overall arrangements of engine head, and show that to overcome this problem a simple solution, like an additional nozzle redirecting the jet towards the piston top, can easily support a correct charge distribution.

References

[1] Kado T. et al., “The Development of 1 MW Class Gas Engine and Its Application to Cogeneration Systems”, 2008, Mitsubishi Heavy Industries, Ltd. Technical Review Vol. 45 No. 1 (Mar. 2008)
[2] Nakai S. et al., “The combustion improvement technologies for large natural gas engine by in-cylinder observation and prediction”, CIMAC Congress 2007, Vienna
[3] Bika A. S.,“Synthesis Gas Use in Internal Combustion Engines”, PhD dissertation, University of Minnesota, 2010
[4] Catapano, F., Di Iorio, S., Sementa, P., and Vaglieco, B., "Characterization of CH_4 and CH_4/H_2 Mixtures Combustion in a Small Displacement Optical Engine", 2013, SAE Int. J. Fuels Lubr., 6(1), pp. 24-33
[5] Baratta, M., D'Ambrosio, S., and Misul, D., "Performance and Emissions of a Turbocharged Spark Ignition Engine Fuelled with CNG and CNG/Hydrogen Blends", 2013, SAE Technical Paper 2013-01-0866
[6] Westport Power Inc., http://www.westport.com/is/core-technologies/fuel-injectors
[7] Shudo T., “Improving thermal efficiency by reducing losses in hydrogen combustion engines”, International Journal of Hydrogen Energy, 2007, vol. 32, pp. 4285-4293
[8] Baratta et al., “Numerical and Experimental Analysis of Mixture Formation and Performance in a Direct Injection CNG Engine”, 2012, SAE Technical Paper 2012-01-0401
[9] Mirmohammadi A., Ommi F., “Simulation a natural gas direct injection stratified charge with spark ignition engine”, International Journal of Automotive Engineering, 2013, vol. 3, n. 3
[10] Jin S. H. et al., “Effect of chamber pressure on the spray from an air-assisted, direct fuel injector”, 5th Asia-Pacific Conference on Combustion, The University of Adelaide, 17-20 July 2005, Adelaide, Australia.
[11] Boretti A. A. et al., “Experimental and Numerical Study of an Air Assisted Fuel Injector for a D.I.S.I. Engine”, 2007, SAE Technical Paper 2007-01-1415
[12] Durbin, P.A., Near-Wall Turbulence Closure Modeling without Damping Functions, Theor. Comput. Fluid Dyn., 1991, 3, 1, pp. 1-13
[13] Durbin, P. A., On the k-e Stagnation Point Anomaly, Int. J. Heat Fluid Flow, 1996, 17, 1, pp. 89-90
[14] Su, H., FIRE Solver Setup, AVL Report, 2006.8.31
[15] Kim G., Kirkpatrick A., Mitchell C., “Computational modeling of natural gas injection in a large bore engine”, ASME Journal of Engineering for Gas Turbines and Power, 2004, vol. 126, pp 656-664
[16] Zanforlin S., et al., “Two step concept for low-pressure direct hydrogen injection”, Proceedings of ASME Internal Combustion Engine Division Fall Technical Conference, 2009, September 27-30, Lucerne, Switzerland
[17] Li Y. et al., “Characteristic and Computational Fluid Dynamics Modeling of High-Pressure Gas Jet Injection”, Transactions of the ASME, Vol. 126, January 2004.